A simple topological index for measuring nonbipartivity in nanostructures

A.V. Luzanov

STC "Institute of Single Crystals", National Academy of Sciences of Ukraine,
60 Nauky Ave., 61001 Kharkiv, Ukraine

We consider a nonbipartivity quantification problem for complex atomistic structures treated as graphs. In simple words, the bipartivity means that the corresponding graph has no odd-membered cycles. Based on preliminary results (2021) we now propose a topological index I_{AS}. By the latter a graph spectral asymmetry is suitably transformed into a size-extensive measure of nonbipartivity. The I_{AS} index ls tested on simple graphs, and compared with other nonbipartivity indexes. For several graph types (cycles, sunlet and wheel graphs etc.) the analytical results are obtained. The focus of our numerical computations is on large-scale nanoclusters (fullerenes with hundreds atoms and nonbipartite defects in graphene nanoclusters). It is emphasized that the size-extensivity of the given measure I_{AS} is principal when analyzing nonbipartivity in quantitative terms.

Keywords: adjacency matrix, parity theorem, cycle-based graphs, vertex frustration, giant fullerenes, nanographenes.

Простий топологічний індекс, що вимірює недводольність у нанокластерах. *А. В. Лузанов*

Досліджено проблему квантифікації недводольності складних атомістичних структур, що розглядаються як графи. В простих термінах дводольність означає, відсутність у відповідному графі циклів непарної довжини. Базуючись на попередніх результатах (2021), ми пропонуємо топологічний індекс недводольності I_{AS}. За допомогою останнього спектральна асиметрія графа трансформується у деяку розмірно узгоджену міру недводольності. Індекс I_{AS} було протестовано й порівняно з іншими індексами недводольності. Отримано аналітичні результати щодо деяких типів графів (цикли, сонечко та колеса тощо). Центр уваги наших чисельних розрахунків становили нанокластери великого розміру (фулерени із сотнями атомів та графенові нанокластери з недводольними дефектами). Акцентовано, що саме розмірна узгодженість запровадженої міри I_{AS} є принциповою в кількісному аналізові недводольності.

1. Introduction

When describing internal structure of complex discrete-like systems, topological techniques are quite appropriate due to their universal applicability [1,2]. In particular, graph-theoretic approaches cover many structural issues in nanophysics as well. There exists one nontrivial problem in the graph-theoretic characterization of complex systems. It is a quantitative treatment of the so-called bipartivity and related nonbipartivity. The problem was

clearly posed in [3] while some important preliminary results were obtained earlier [4].

Recall that the graph bipartivity simply means that the graph possesses no odd-cycles. A direct count of odd-cycles is not trivial for large-scale networks, and various schemes were invented for analyzing bipartivity and nonbipartivity in quantitative terms (e.g., see references [5-9]). Recently, the nonbipartivity measures were also discussed for conjugated carbon-containing π-structures [10] (in the last

appendix of loc. cit.). A quite simple approach has been given therein, but only few examples were presented. Thus, real possibilities of our approach remained unclear. The purpose of the paper is to elucidate these points by the extended graph-theoretic consideration of middle and large scale networks.

2. How to measure nonbipartivity

The simplest basic notions of graph theory are assumed to be familiar to the reader, and we only recall some specific terms. Considering any atomistic structure in the graph-theoretic terms, one treats atomic centers as graph vertices, and interatomic bonds as graph edges. In this approach the basic is a graph adjacency matrix A with matrix elements $A_{ij} = 1$ if vertices i and j are connected by an edge, otherwise $A_{ij} = 0$. Notice that this definition is quite similar to that commonly defined in the Hueckel π-electron theory of conjugated carbon-containing systems (then $(-A)$ is interpreted as the modeled one-electron Hamiltonian). Matrix A is frequently termed a topological matrix.

Likewise, the important graph-theoretic notion of bipartite graph has an analogous one in the Hueckel theory where the so-called alternant systems are defined [11]. Namely, the graph is bipartite (or two-coloring) if its vertices can be colored by two different colors in such a way that no neighboring (adjacent) vertices are colored identically. The strictly equivalent requirement is an absence of odd-cycles in any bipartite graph and in alternant system respectively. Various formal definitions and corresponding algorithms were proposed for estimating the graph bipartivity and nonbipartivity (see review [9]). Here we focus on two popular approaches which are computationally relatively undemanding.

The first algorithm is based on a spectral analysis of the special matrix named the signless Laplacian Q. Let us define the diagonal matrix D in which the i-th diagonal element D_{ii} is equal to the number of neighboring vertices of the i-th vertex (vertex degree). Then, by definition

$$Q = D + A \cdot \tag{1}$$

The remarkable property of Q is that its smallest eigenvalue, μ_{min}, is zero if and only if the connected graph is bipartite [4,12]. Thence, the deviation of μ_{min} from zero is a possible measure of nonbipartivity.

Another frequently used method which was given in [6], invokes only the A-spectrum, that is the adjacency matrix eigenvalues $\{\lambda_j\}$, where $1 \leq j \leq N$, and N is a total number of vertices. The appropriate nonbipartivity measure can be written in the form of the following index:

$$I_{Estr} = 2 \, \text{Tr}[\sinh(A)] / \text{Tr}[\exp(A)] \tag{2}$$

with $\exp(A)$ and $\sinh(A)$ being the standard matrix functions. This measure obeys the inequality: $0 \leq I_{Estr} \leq 1$, so the value $I_{Estr} = 1$ corresponds to maximally nonbipartite graphs. In [6] the corresponding bipartivity quantification scheme was motivated by a consistent random-walk analysis on graphs. In our study we will explore primarily the new approach [10] where a spectral asymmetry of A is directly taken as the source of nonbipartivity measures.

3. Spectral asymmetry as a nonbipartivity measure

Seemingly, for bipartite systems the special symmetry of A-spectrum was first founded by Coulson and Rushbrooke in [11]. From their parity theorem we have the following symmetry relation:

$$\lambda_j = -\lambda_{N-j+1}, \tag{3}$$

that is applicable for all N eigenvalues λ_j of A. This relation is strongly valid for bipartite systems only (theorem 2.3.4 in [12]). It suggests the idea [10] that an admissible nonbipartivity measure can be simply constructed in terms of individual spectral asymmetries. Let us denote by σ_j the asymmetry contribution from the given λ_j. Explicitly, we set

$$\sigma_j = |\lambda_j + \lambda_{N-j+1}|, \quad 1 \leq j \leq N, \tag{4}$$
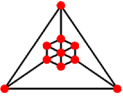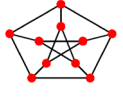
so that $\sigma_j = \sigma_{N-j+1}$. Next, we take all such σ_j with an equal weight, and it produces (up to a factor) the appropriate nonbipartivity measure proposed in [10]. Signifying this measure by I_{AS}, we define:

$$I_{AS} = \frac{1}{4} \sum_{1 \leq j \leq N} \sigma_j. \tag{5}$$

In Eq. (5) a factor $\frac{1}{4}$ is included for convenience (this will be seen below). Evidently, $I_{AS} = 0$ if and only if the system under study is bipartite.

To verify the method let us take first the triangle graph C_3 as a simplest nonbipartite structure. For this graph, the set {-1, -1, 2} is its A-spectrum, and {1, 1, 4} is its Q-matrix spectrum. Then, $I_{AS} = \mu_{min} = 1$ for C_3. This fact al-

Table 1. Comparison between nonbipartivity measures I_{Estr}, μ_{min}, and I_{AS} for typical graphs.

Graph	I_{Estr}	μ_{min}	I_{AS}
C_3	0.314	1	1
C_5	0.108	0.382	1
C_7	0.002	0.198	1
(Golumb)	0.526	1.316	1.874
(Petersen)	0.082	1	3
K_8	0.982	6	6
K_9	0.992	7	7

lows us to adopt that by using the indexes I_{AS} we evaluate nonbipartivity in "triangle units". In Table 1 we present the results for some typical cyclic graphs.

To start we consider simple unicyclic graphs C_N having N vertices ($N = 3$, 5 and 7 in Table 1). Furthermore, more sophisticated graphs are also studied here. These are the well-known Petersen graph (p. 225 in [13]), the Golumb graph, and the complete graphs K_8 and K_9. Recall that complete graph K_N is the graph in which all N vertices are connected between themselves. Using the known A-spectrum of K_N, ([14]. p. 115]) we find that $I_{AS} = \mu_{min} = N - 2$. It implies that the nonbipartivity is large, increasing linearly: $I_{AS}[K_N] \to N$. It is a natural result which reflects an extremal nonbipartivity of K_N having all possible odd-cyclic subgraphs. Notice that the identity $I_{AS} = \mu_{min}$ (as in the the above examples) is seldom valid.

Particularly, we see from Table 1 that even for elementary graphs such as C_N the behavior of different nonbipartivity indexes is quite distinctive. For instance, the $E_{str.}$ index falls off too quickly with increasing the cycle size. The μ_{min} measure also decreases, only more slowly, whereas the new I_{AS} index is independent of the odd-cycle size. The Petersen graph again demonstrates the too low value of I_{Estr} (even lesser than for C_3). At the same time, rather large nonbipartivity measures should be expected intuitively in case of the intricate Petersen graph.

The above dissimilarity is partly rooted in a specific problem of size-consistency of nonbipartivity measures (for the size-consistency notions see, e.g. [15,16]) . Really, μ_{min} and I_{Estr} are size-intensive quantities (like ionization potentials). It means that these ones are the same for the given graph and for a ensemble of disconnected identical copies of the graph. Note that another possible index [9] is based on fraction $\lambda_{min}/\lambda_{max}$, namely, $1 - |\lambda_{min}/\lambda_{max}|$, and it is also size-intensive. Unlike these three indexes, I_{AS} is actually the size-extensive (additively separable) characteristic like total energy. More exactly, I_{AS} possesses only the homogeneous additivity related to ensembles of identical species. Then, I_{AS} and the both μ_{min} and I_{Estr} measures are essentially distinct in their nature, and therefore the results given by I_{AS} and the rest indexes are highly disparate. Judging from the above-given data, it seems that the I_{AS} measure can serve as a more suitable tool for comparable studies, especially in case of large-scale structures. Thus, in what follows we will focus mainly on investigating nonbipartivity by means of I_{AS}, giving other indexes from time to time.

4. Cycle-based structures

We now describe more systematically the results obtained for several typical problems having the cyclic graph as a core subgraph. Let us return to the unicyclic graph C_N with arbitrary N. In chemistry of conjugated systems, C_N corresponds to cyclic polyenes for which many analytical results were produced. As will be seen below, the same is possible for topological nonbipartivity indexes.

Due to the cyclic symmetry of C_N, its well-known A-spectrum is to be

$$\lambda_j[C_N] = 2\cos[2\pi j/N], \quad 0 \le j \le N-1 . \quad (6)$$

The Q-matrix spectrum for C_N trivially follows from the A-spectrum, so that for any even $N=2n$, that is for bipartite cycle, one has $\mu_{min} = I_{AS} = 0$. In the case of odd-cycles ($N=2n+1$), we obtain $\mu_{min} = 2(1 - \cos[2\pi/N])$, which for large N decreases as $(\rho/N)^2$. Opposite to this, the equality

$$I_{AS} = 1 \qquad (7)$$

is true for any odd-cycle, as can be anticipated from examples in Table 1.

Here, we only briefly sketch the proof of this nonevident identity. To this end, we need to rearrange the A-spectrum in Eq. (4) before using

the definition of .., Eq. (5). A suitable form of Eq. (5) for spectrum (6) is

$$I_{AS} = \sum_{j=0}^{n} |\cos[2\pi j / (2n+1) + \cos[2\pi(n-j)/(2n+1)]| \tag{8}$$

By usual trigonometry we can rewrite it (up to a factor) in the form containing the standard sum of cosines of angles in arithmetic progression, and it lead us easily to Eq. (7). Stress that in terms of index I_{AS}, any C_{2n+1} has the same nonbipartivity as the triangle C_3. While this fact may seem surprising, it should be noted that the same constant value is assigned to all odd cycles in the known vertex frustration method [8]. In the latter, one identifies a nonbipartivity index with a minimal number of vertices deleting which converts the given graph into a bipartite graph (for more results see the Appendix).

As the next step, consider one special (sunlet) graph which has C_N as a leading subgraph. The sunlet graph can be constructed by attaching a single pendant vertex to each vertex on C_N. We will name such the graphs by radialenes (as in chemistry) and denote them by R_N. The radialene A-spectrum is known long ago [17]. By using this we find that the needed individual asymmetry contributions, Eq. (4), are the same as in C_N, and the resulting expression for our nonbipartivity measure is immediately reduced to Eq. (8). Then, Eq. (7) giving for C_N the N-independence of I_{AS} is also valid for R_N. Similarly, the behavior of μ_{min} in the R_N graphs almost reproduces that of C_N, namely, with enlarging N the μ_{min}-nonbipartivity of radialenes decreases asymptotically as $(\pi/N)^2/2$.

Next, the prism graph, P_N with $2N$ vertices has two subgraphs C_N. The A-spectrum P_N is simply computed, and can be represented in terms of Eq. (6) to be $\{\lambda_j[C_N]+1, \lambda_j[C_N]-1\}$ (see [13], p. 306). However, these two eigenvalue subsets overlap considerably, and we could not obtain I_{AS} analytically. The numerical data are displayed in Table 2 where the results for the conventional wheel graph W_N are also included.

In the wheel graph, each vertex of the associated C_{N-1} graph is linked to the central singleton graph K_1 to form a counterpart of a spoked wheel. The main analytical results for W_N are as follows [14]: the A-spectrum contains the same A-eigenvalues as the subgraph C_{N-1} together with two additional numbers $1+\sqrt{N-1}$ and $1-\sqrt{N-1}$. Due to these two

Table 2. Comparison between nonbipartivity measures μ_{min} and I_{AS} for prism and wheel graphs.

Prism	μ_{min}	I_{AS}	Wheel	μ_{min}	I_{AS}
P_3	1	1	W_4	2	2
P_5	0.382	1.764	W_5	1	1.238
P_7	0.198	1.494	W_6	1.382	1.831
P_9	0.121	1.241	W_7	1	1.646
P_{11}	0.081	1.746	W_8	1.198	2
P_{13}	0.058	1.413	W_9	1	2

eigenvalues, Eq. (7) for small N is not valid because of intruding $\{1+\sqrt{N-1}, 1-\sqrt{N-1}.\}$ into spectrum $\{\lambda_j[C_{N-1}]\}$. With this, we have

$$I_{AS} = 2 \tag{9}$$

for W_4 (as in the formal case of two disconnected triangles), but lesser values for few subsequent wheel graphs up to W_7 only. All further members of this series (W_8 etc.) exactly follow Eq. (9) for W_4. Thus, for the wheel graphs of not too small size the I_{AS} measure is equal again to the constant value, and, importantly, twice the I_{AS} value for C_N. The fact that the nonbipartivity of wheel graphs is certainly larger than that of C_N seems quite natural if applying intuitive reasoning. It is interesting that the vertex frustration method in fact provides the same picture (see the Appendix).

It is also worth discuss the behavior of the μ_{min} measure in W_N. As seen from Table 2, μ_{min} for W_{2n} leads to almost the same values $\mu_{min}=1$ as for the one triangle. For odd wheel graphs W_{2n+1} Eq. (9) is exact for all $n>7$. We see that by using μ_{min}, one can underestimate the nonbipartivity even in comparably simple structures.

To conclude this section we briefly analyze the results obtained for the Moebius ladder, M_N, with even $N=2n$. Recall that M_{2n} is produced from the prism graph P_{2n} by making one twist in a set of the edges which link two subgraphs C_n in P_{2n}. It is also known that, unlike C_n, the Moebius ladder is bipartite only for odd n. Therefore we will work here only with the even n case. The A-spectrum of M_{2n} was frequently discussed, and a suitable representation is given in [13], p. 75. It allows us to yield the formally same expression for μ_{min} as for C_n (see the above text after Eq. (6)). But for I_{AS} the simple result, Eq. (7), is not valid for M_{2n}. It can be seen from the following numerical data for I_{AS} in M_{2n} with $n=2,4,6,8$, and 10, namely, 2, 1.41, 1.28, 1.68, and 1.51, respectively. For

Table 3. Nonbipartivity measures μ_{min} and I_{AS} for Platonic solids.

Solid	N	Faces	I_{Estr}	μ_{min}	I_{AS}
T_h	4	4{3}	0.62	2	2
O_h	6	8{3}	0.68	2	2
I_h	12	20{3}	0.72	2.76	4
$I_h[D]$	20	12{5}	0.42	0.76	3

greater even n values, numerical variations slowly oscillate, and I_{AS} goes to 3/2. Summing this section, we may suggest that the proposed index I_{AS} can serve as a reliable tool for studying nonbipartivity in arbitrarily complex systems.

5. Fullerenes and giant icosahedral structures

Fullerenes and related structures were extensively studied by various graph-theoretical approaches ([18-20] and many others), In particular, the quantitative bipartivity of fullerene structures was also discussed, e.g. in [21-23]. It is interesting to consider the same problem by invoking our nonbipartivity measure I_{AS}, which, we recall, has a suitable size-dependence behavior like the graph energy. It is sensible to start with the Platonic and Archimedean solids which are the fullerene predecessors in classical geometry. The needed structural and geometrical data were taken from [24,25].

Among the Platonic N-hedrons (polyhedra), only cube ($N = 6$) is bipartite. In Table 3 we present the numerical date for the rest N values: tetrahedron (T_d), octahedron (O_h), icosahedron (I_h), and dodecahedron ($I_h[D]$). These shorthands are used in the table. Just note that μ_{min} again underestimates the nonbipartivity, particularly in the case of icosahedron. The discrepancy is only strengthened in the Archimedean polyhedra, such as truncated dodecahedron and others. The results for large-scale

Archimedean solids and giant fullerenes are presented in Tables 4 and 5. For several basic structures from these tables it is possible to make comparison with the vertex frustration approach (see the Appendix).

When inspecting Table 4, it becomes seemingly apparent that both the indexes, I_{Estr} and μ_{min}, are unsatisfactory for quantifying nonbipartivity in the Archimedean solids. The snub dodecahedron is a particularly striking example in this respect. In the case we have 12 pentagons surrounded by 80 triangles, so no surprise that we obtain the very large I_{AS} = 16.6. At the same time, μ_{min} and I_{Estr} cannot provide the needed sharp nonbipartivity discrimination, say, between the snub cube and snub dodecahedron.

Now we discuss the results of Table 5 for the fullerene family. In order to distinct N-atomic carbon fullerenes from N-cycles C_N we will designate the first by symbol [CN]. In the graph-theoretic terms any fullerene can be treated as a plane graph consisting of exactly 12 pentagons surrounded by hexagons. In case of the fully isolated 12 pentagons one should obtain the resulting $I_{AS} = 12$ because Eq. (7) is valid for the single pentagon. However, the behavior of even one pentagon in hexagonal (graphene-like) domain is not simple (it will be considered in detail in the next section). For two pentagon substructures which are closely situated inside a small bipartite graphene flake, the total nonbipartivity significantly decreases and attains nearly 0.85 (instead of being 2 for two disconnected cycles C_5). No wonder that in the basic fullerene [C60] we have almost a trice smaller I_{AS} value than the simple additivity rule requires.

Likewise, other middle-size fullerenes only slightly differ from [C60] in respect of nonbipartivity. For instance, the icosahedral [C80] is still less bipartite than [C60]. Judging from Table 5, just too large fullerenes ([C500] and larger ones) can attain $I_{AS} > 5$, that is not so

Table 4. Various nonbipartivity measures for Archimedean solids

Solid	N	Faces	I_{Estr}	μ_{min}	I_{AS}
Truncated Cube	24	8{3}+6{8}	0.28	1	3.56
Rhombicub-octahedron	24	8{3}+18{4}	0.28	1	3
Snub Cube	24	24{3}+6{4}	0.68	2.27	6.12
Snub Dodeca-hedron	60	80{3}+12{5}	0.66	2.44	16.58
Truncated Dodecahedron	60	20{3}+12{10}	0.28	1	8.24
Truncated Icosahedron	60	12{5}+20{6}	0.02	0.38	4.19

Table 5. Nonbipartivity measure I_{AS} for fullerenes [C*N*]. The symmetry group is given in parentheses.

Fullerene	I_{AS}	Fullerene	I_{AS}
[C60] (I$_h$)	4.19	[C320] (I$_h$)	4.72
]C70] (D$_{5h}$)	3.87	[C500] (I$_h$)	5.50
]C76] (D$_2$)	3.44	[C540] (I$_h$)	5.69
]C78] (D$_3$)	3.36	[C720] (I$_h$)	5.62
[C80] (I$_h$)	3.91	[C740] (I)	5.68
[C180] (I$_h$)	4.47	[C860] (I)	5.60
[C240] (I$_h$)	4.63	[C980] (I$_h$)	5.64
[C260] (I)	4.55	[C1500] (I$_h$)	5.61

Table 6. I_{AS} index for the single C$_n$ defect (with n=3,5,7,9) inside nanographene formed by ν hexagon layers.

$\nu \setminus n$	3	5	7	9
1	1.46	1,27	0.74	1.21
2	1.67	1.73	1.07	1.45
3	1.62	1.69	1.17	1.48
6	1.61	1.78	1.63	1.50
7	1.59	1.79	1.56	1.71

great for structures involving 12 pentagons. Thus, in an average, the nonbipartivity of any pentagon in a hexagonal environment of (approximately) one hundred "bipartite" vertices is markedly suppressed in giant fullerene structures with thousands carbon atoms.

In addition, the prefullerene structures shown in Figure 1 demonstrate a nontrivial behaviour of I_{AS} for six-linked pentagon structures. In this figure the first system [C30] is half the buckyball described in [26], and independently within π-electron theories in [27] (under name "the Fuller dome"). Two other systems represent the realistic chemical substances recently synthesized [28]. From the data given in Fig. 1 we see a non-monotonic variation of nonbipartivity in the prefullerene series.

6. Bipartite domains with nonbipartite defect

Here we study numerically the above-mentioned problem how nonbipartivity varies when the given nonbipartite graph becomes a subgraph inside bipartite domain. As a suitable example modeling such situations we treat first the odd-cyclic subgraph C$_n$ immersed into a sufficiently large graphene-like graph (condensed-hexagons). Specifically, we have investigated odd cycles C$_n$ with $n = 3 \div 9$. In this problem, the odd cycles are surrounded by several, generally ν, coordination layers formed by hexagons. The results for various ν and n values are displayed in Table 6. In Table 7 we show, in particular, the carbon-contained structure for ν=2 and n=5, that is the single pentagon defect encircled by two hexagons layers (the first cluster [C45] in Table 7).

Inspecting Table 6 we see that I_{AS} markedly differs from the starting unity value, Eq. (7). The influence of the bipartite environment can be negative, as well as positive, leading to roughly twice the initial unity value. Our experience shows that it is difficult to predict nonbipartivity variations even qualitatively. Table 7 presents additional results for two pentagonal defects in small graphene domains (clusters [C64] and [C96]).

In this context, the interesting example is provided by the pentagonal defects which were

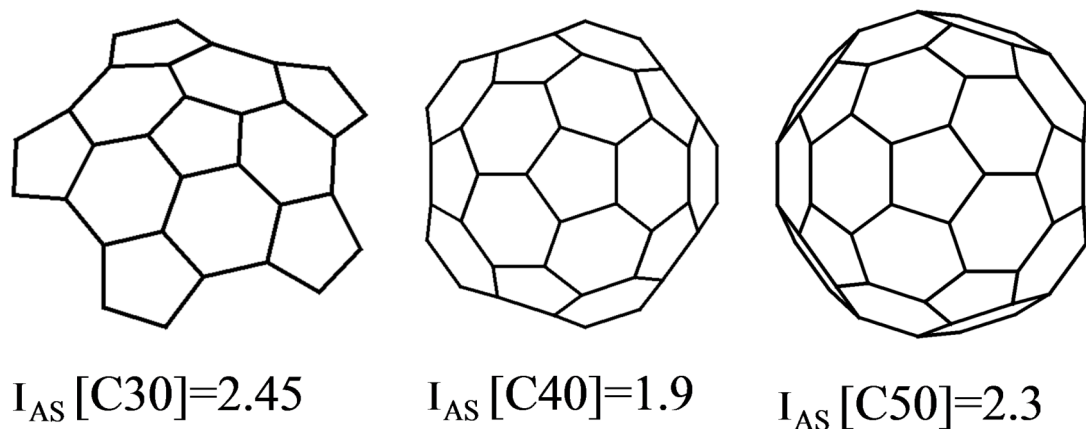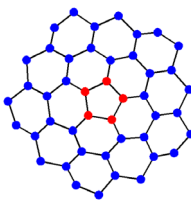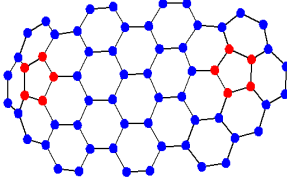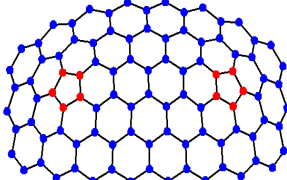I_{AS} [C30]=2.45 I_{AS} [C40]=1.9 I_{AS} [C50]=2.3

Fig. 1. Prefullerene carbon clusters modeled by the five pentagons linked via hexagons.

Table 7. Nonbipartivity measures μ_{min} and I_{AS} for the single and double pentagonal defects (colored in red) inside small graphene nanoclusters.
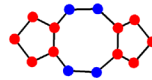
Cluster	μ_{min}	I_{AS}
[C45]	0.052	1.729
[C64]	0.046	0.850
[C96]	0.046	0.998

Table 8. The I_{AS} index for the isolated nonbipartite defect [C14] and three large-scale PA graphene nanoclusters containing the same defect.

Basic Structure	Cluster	I_{AS}
	[C14]	0.989
PA[7a,7z]	[C116]	0.716
PA[15a,8z]	[C494]	0.997
PA[21a,12z]	[C1030]	1.016

studied quantum chemically in [29] for finite-sized periacene structures (PA). In the cited work, the so-called (*ia,jz*) PA with *i=j*=7 were treated. After removing two carbon atoms (for doing carbon divacancy) the authors have produced the relaxed geometry of the structure with a defect (see the figure 1e in [29]). Their nanographene cluster included 116 carbon atoms involving the basic nonbipartite dipentagon-octagon substructure (the latter is displayed as the first system [C14] in our Table 8). In Table 8, we also considered graph-theoretically more extended PA, [C494] and [C1030] systems with the same nonbipartite defect. For the studied systems, we again observe a non-monotonic variation of the nonbipartivity even for surroundings with hundreds and thousand carbon atoms.

8. Conclusion

Summing up, we have characterized nonbipartivity of structurally complex systems by the new topological index I_{AS}, Eqs. (4) and (5), derived from a spectral asymmetry of corresponding adjacency matrix. The I_{AS} index is in fact the size-extensive (like total energy) topological measure. It makes I_{AS} a suitable tool for comparable analysis among nonbipartite structures with basically different size. At the same time,

many of existing bipartivity or nonbipartivity measures are not easy to be used for comparison aids because usually they possess a size-intensivity, and may produce sharply decreased values with increasing size. By using I_{AS} we can reasonably treat nonbipartivity in large nanoclusters with up to thousand and more atoms as it shows the giant fullerenes in Table 5. Interestingly, the most fullerenes under study are rather similar as to their bipartivity, albeit many of them are much larger (yet more than ten times) than the reference [C60] structute. In the same fashion we also studied the related problem of nonbipartite defects inside modeled bipartite graphene-like lattices. The main conclusion we can made now is that additive indexes, such as I_{AS} and the vertex frustration index [7], seem to be preferable. Nonetheless, the comparison between these additive measures (see the Appendix) demonstrates that it is hard to reach full quantitative agreement in describing nonbipartivity of complex systems.

Additional investigations should be made to elucidate some principal points. One of them is an origin of increasing and decreasing nonbipartivity in special bipartite domains surrounding nonbipartite defects (section 6). This and supplementary issues, e.g. exploring bipartivity in complex crystal-like structures (see [32]) and in the finite-size frustrated spin magnets (as in [33]), are supposed to be scrutinized in future.

Appendix. *Comparison with the vertex frustration measure*

Recall that in the vertex frustration (vertex bipartization) approach [7,23,30] one must find, for the given graph, a minimal number I_{VF} of the graph vertices such that removing them makes the resulting graph bipartite. The method is very tricky to be performed generally, but the problem can be clearly tractable for some graph types. For instance, the result

is evident for odd cycles: $I_{VF}[C_N]=1$ for any odd N, that is the same as in Eq. (7). Simply obtained summary data for I_{VF} are as follows. In the notation of the main text, we have, for the cycle-based graph set $\{C_{2n+1}, R_{2n+1}, W_{2n+1}, P_N\}$ the corresponding I_{VF} set is $\{1, 1, 2, 2\}$. In addition, $I_{VF}=3$ for the both Golumn and Petersen graphs. In case of the Platonic solids $\{T_d, O_h, I_h, I_h[D]\}$ we obtain $I_{VF}=\{2, 2, 6, 6\}$. Comparing the above with the respective data of Tables 1-3 we observe the coincidence or a certain similarity of the results. Furthermore, $I_{VF}=I_{AS}=N-2$ for the complete graph K_N.

As the last examples of the close similarity between I_{VF} and I_{AS} indexes we shortly discuss our computations for the friendship and sunflower graphs (F_N and Sf_N in usual notation). In case of the F_N graph we can use its A-spectrum from [31] that gives us the full coincidence: $I_{VF}=I_{AS}=1$. The sunflower graph provides a more interesting situation. This graph can be derived from the wheel graph W_N by attaching a single vertex s_j to each vertex v_j of the C_N subgraph of W_N. In doing so one must link s_j with v_j and v_{j+1}. Turning to the I_{VF} measure for Sf_N we easily find I_{VF} for small N in Sf_N. Namely, $I_{VF}[Sf[3]]=I_{VF}[Sf[4]]=3$, Generally we find that $I_{VF}[Sf_{2n-1}]=I_{VF}[Sf_{2n}]=n$. This means that for large N the I_{VF} index is linear in N:

$$I_{VF}[Sf_N] \to N/2.$$

It can be compared with the analogous I_{AS} results for small N: $I_{AS}[Sf[3]]=I_{AS}[Sf[4]]=3$. For large N the numerical data are only available. They give us an approximate asymptotic which is linear in N. Namely, $I_{AS}[Sf[N] \to 0.415\,N$ that is sufficiently close to the above result for I_{VF}.

All these facts are not accident because like I_{AS} the I_{VF} index is the additive, or more exactly, additively separable measure, as stated by the Lemma 1 in [7]. It must be underlined that in our opinion the additivity property is warranted when comparing nonbipartivity even between middle-size systems.

However, for fullerenes the I_{AS} and I_{VF} data do not provide a good concordance. According to [30], $I_{VF}[C60]=12$, and the same I_{VF} value is true for the related fullerene structures with $N=12\,(2n+1)$. Then, based on [30], one also has the high value $I_{VF}=12$ for [C180], [C540], and [C1500]. More than that, one can obtain the I_{VF} values markedly higher than those of the I_{AS} approach even for simple systems as the

example of the defect [C14] in Table 8 shows this: $I_{VF}[C14]=2$. All this illustrates that it is difficult to uniquely and universally define the topological nonbipartivity in quantitative terms.

References

1. S.N.Dorogovtsev, J.F.F.Mendes, Evolution of Networks: From Biological Nets to the Internet and WWW, Oxford University Press, New York (2003).

2. E.Estrada, The structure of complex networks: theory and applications, Oxford University Press, Oxford (2016).

3. P.Holme, F.Liljeros, C.R.Edling, B.J.Kim, Phys. Rev. E, 68, 6653 (2003). https://doi.org/10.1103/PhysRevE.68.056107 .

4. M.Desai, V.Rao, *J. Graph Theory*, **18**, 181 (1994). https://doi.org/10.1002/jgt.3190180210 .

5. E.Estrada, J.A.Rodríguez-Velázquez, *Phys. Rev. E*, **72**, 056103 (2005); E.Estrada, *SeMA*, **79**, 57 (2022). https://doi.org/10.1103/PhysRevE.72.046105 .

6. T.Pisanski, M.Randic, *Discrete Appl. Math.*, **158**, 1936 (2010). https://doi.org/10.1016/j.dam.2010.08.004 .

7. Z.Yarahmadi, A.R.Ashrafi, *Appl. Math. Lett.*, **24**, 1774 (2011). https://doi.org/10.1016/j.aml.2011.04.022 .

8. S.Hayat, A.Khan, F.Yousafzai, M.Imran, *Optoelectron. Adv. Mater. Rapid Commun.*, **9**, 869 (2015).

9. J.Kunegis, *Internet Math*, **11**, 201 (2015). https://doi.org/10.1080/15427951.2014.958250

10. A.V.Luzanov, *Kharkiv University Bulletin, Chem. Ser.*, **32** (55), 6 (2019). https://doi.org/10.26565/2220-637X-2019-32-01 .

11. C.A.Coulson, G.S.Rushbrooke, *Proc. Cambr. Phil. Soc.*, **36**, 193 (1940). https://doi.org/10.1017/S0305004100017163 .

12. A.S.Asratian, T.M.J.Denley, R.Haggkvist, Bipartite Graphs and their Applications; Cambridge University Press: Cambridge (1998).

13 D.Cvetkovic', M.Doob, H.Sachs, Spectra of Graphs - Theory and Application, Acad. Press, New York (1980).

14. P.V. Mieghem, Graph Spectra for Complex Networks, Cambr. University Press, Cambridge (2011).

15. J.A.Pople, *Rev. Mod. Phys.*, **71**, 1267 (1999). https://doi.org/10.1103/RevModPhys.71.1267 .

16. M.Deleuze, J.Delhalle, B.T.Pickup, J.L.Calais, *Adv. Quantum. Chem.*, **26**, 35 (1995). https://doi.org/10.1016/S0065-3276(08)60111-2 .

17. I.Gutman, N.Trinajstić and T.Živković, *Croat. Chem. Acta*, **44**, 501 (1972).

18. F.Cataldo, A.Graovac, O. Ori, The Mathematics and Topology of Fullerenes, Springer, Berlin (2011).

19. P.Schwerdtfeger, L.Wirz, J.Avery, *WIRE Comput. Mol. Sci.*, **5**, 96 (2015). https://doi.org/10.1002/wcms.1207 .

20. V.Andova, F.Kardoš, R.Škrekovski, *Ars Mathematica Contemporanea*, **11**, 353 (2016). https://hal.science/hal-01416354/document .

21. T. Došlić, *Chem. Phys. Lett.*, **412**, 336 (2005). https://doi.org/10.1016/j.cplett.2005.07.013; T.Došlić, D.Vukičević, *Discrete Appl. Math.*, **155**, 1294 (2007). https://doi.org/10.1016/j.dam.2006.12.003 .

22. L.Faria, S.Klein, M.Stehlík, *SIAM J. Discrete Math.*, **26**, 1458 (2012). https://doi.org/10.1137/120870463 .

23. Z.Yarahmadi, A.R.Ashrafi, *Electr.on. Notes Discrete Math.*, **45**, 107 (2014).

24. http://dmccooey.com/polyhedra/index.html .

25. https://nanotube.msu.edu/fullerene/ .

26. D.J.Klein, X.Liu, *J. Math. Chem.*, **11**, 199 (1992). https://doi.org/10.1007/BF01164204 .

27. G.E.Vaiman, G.T.Klimko, M.M.Mestechkin, *Theor. Exp. Chem.*, **29**, 143 (1993) https://doi.org/10.1007/BF00531169 .

28. E.A.Jackson, B.D.Steinberg, M.Bancu et al, *J. Am. Chem. Soc.*, **129**, 484 (2007). https://doi.org/10.1021/ja067487h ; L.T.Scott, E.A.Jackson, B.D. Steinberg et al, *J. Am. Chem. Soc.*, **134**, 107 (2012). https://doi.org/10.1021/ja209461g .

29. M.Pinheiro Jr, D.V.V.Cardoso, A.J.A.Aquino, et al., *Mol. Phys.*, **117**, 1519 (2019). https://doi.org/10.1080/00268976.2019.1567848 .

30. A.R.Ashrafi, M.A.Iranmanesh, Z.Yarahmadi, in Topological Modelling of Nanostructures and Extended Systems (Carbon Materials: Chemistry and Physics), ed. by A.R.Ashrafi, Springer, New York (2013), p.473. https://link.springer.com/chapter/10.1007/978-94-007-6413-2_14

31. A.Abdollahi, S.Janbaz, *Trans. Combinatorics*, **3**, 17 (2014). https://doi.org/10.22108/toc.2014.4975 .

32. J.C.Navarro-Munoz, R.López-Sandoval, M.E.García, *J. Phys. A*, **42**, 315302 (2009). https://iopscience.iop.org/article/10.1088/1751-8113/42/31/315302 .

33. W.Florek, G.Kamieniarz, A.Marlewski, *Phys. Rev. B*, **100**, 054434 (2019). https://doi.org/10.1103/PhysRevB.100.054434 .